NADPH Oxidase 4 Contributes to Transformation Phenotype of Melanoma Cells by Regulating G_2-M Cell Cycle Progression

Maki Yamaura,[1] Junji Mitsushita,[2] Shuichi Furuta,[2] Yukiko Kiniwa,[1] Atsuko Ashida,[1] Yasuhumi Goto,[1] Wei H. Shang,[2] Makoto Kubodera,[2] Masayoshi Kato,[2] Minoru Takata,[1] Toshiaki Saida,[1] and Tohru Kamata[2]

Departments of [1]Dermatology and [2]Molecular Biology and Biochemistry, Shinshu University Graduate School of Medicine, Matsumoto, Nagano, Japan

Abstract

Generation of reactive oxygen species (ROS) has been implicated in carcinogenic development of melanoma, but the underlying molecular mechanism has not been fully elucidated. We studied the expression and function of the superoxide-generating NADPH oxidase (Nox)4 in human melanoma cells. Nox4 was up-regulated in 13 of 20 melanoma cell lines tested. Silencing of Nox4 expression in melanoma MM-BP cells by small interfering RNAs decreased ROS production and thereby inhibited anchorage-independent cell growth and tumorigenecity in nude mice. Consistently, a general Nox inhibitor, diphenylene iodonium, and antioxidants vitamine E and pyrrolidine dithiocarbamate blocked cell proliferation of MM-BP cells. Flow cytometric analysis indicated that Nox4 small interfering RNAs and diphenylene iodonium induced G_2-M cell cycle arrest, which was also observed with another melanoma cell line, 928mel. This was accompanied by induction of the Tyr-15 phosphorylated, inactive form of cyclin-dependent kinase 1 (a hallmark of G_2-M checkpoint) and hyperphosphorylation of cdc25c leading to its increased binding to 14-3-3 proteins. Ectopic expression of catalase, a scavenger of ROS, also caused accumulation of cells in G_2-M phase. Immunohistochemistry revealed that expression of Nox4 was detected in 31.0% of 13 melanoma patients samples, suggesting the association of Nox4 expression with some steps of melanoma development. The findings suggest that Nox4-generated ROS are required for transformation phenotype of melanoma cells and contribute to melanoma growth through regulation of G_2-M cell cycle progression. [Cancer Res 2009;69(6):2647–54]

Introduction

A growing body of evidence indicates that reactive oxygen species (ROS) generated by NADPH oxidase (Nox) family enzymes [Nox1-5 and dual oxidases (Duox1 and 2)] play critical roles in various physiologic processes in *Caenorhabditis elegans* as well as mammals (1). These include innate immunity, cell growth, and apoptosis. For example, Nox1 mediates angiotensin II-induced proliferation of vascular smooth muscle cells (2) and platelet-derived growth factor– or epidermal growth factor–dependent mitogenesis of nonphagocytic cells (3, 4). Nox4 is integrated into the receptor systems for insulin-induced glucose transport (5) and lipopolysaccharide-stimulated inflammation (6). The NADPH oxidase consists of multiple subunits including a Nox family protein, the catalytic moiety homologous to phagocytic gp91phox, and regulatory proteins. It catalyzes reduction of molecular oxygen to produce superoxide and its metabolite, hydrogen peroxide.

It has been known that ROS are spontaneously generated in malignant cancer cells, but their origin and biological meaning remained obscured (7). Recent studies revealed some aspects of the functional relationships between Nox family genes and increased ROS production in tumor cells. Nox1-generated ROS are functionally required for oncogenic Ras transformation phenotype including anchorage-independent growth and tumorigenesis (4, 8). Nox4 contributes to cell survival of pancreatic cancer cells, and this survival signaling seemed to be mediated by the impared activities of AKT and its target ASK1 (9, 10). Nox5 has also been implicated in cell viability of prostate cancer cells (11) and Barrett esophageal adenocarcinoma cells (12).

Melanoma is one of the aggressive tumors with a high frequency of metastasis and malignancy in melanoma cells is often accompanied by elevated ROS production through multiple mechanisms (13). Overexpression of the antioxidant enzyme, superoxide dismutase, suppresses the ability of melanoma cells to form colonies in soft agar as well as tumors in nude mice (14). The dietary antioxidant, tocopherol (vitamine E), induces growth inhibition of melanoma cells (15). These observations imply that redox alterations play an important role in the carcinogenic evolution of melanoma. With the respect to involvement of Nox isozymes in these ROS productions, Nox1 has been implicated in acute ROS formation in human kerationcytes elicited by UV A radiation (16), whose role in development of cutanous melanoma is still being debated. Recently, Nox4 expression was reported to be constitutively up-regulated and partially account for the elevated ROS production in some of melanoma cell lines (17), but the Nox4 action has not been fully elucidated. In the present study, we describe that ablation of Nox4 expression by RNA interference blocks both proliferation of melanoma cells and tumorigenesis derived from melanoma cells in athymic nude mice. This growth inhibition seems to be a consequence of inhibition of G_2-M cell cycle transition, which is associated with increased phosphorylation of cyclin-dependent kinase 1 (CDK1), a key mitosis-promoting kinase and hyperphosphorylation of cdc25c. Furthermore, up-regulated expression of Nox4 was detected in some of melanoma samples isolated from patients. Our finding suggests that Nox4-generated ROS exert a mediating role in melanoma cell growth by regulating G_2-M cell cycle progression and for the first time

Note: Supplementary data for this article are available at Cancer Research Online (http://cancerres.aacrjournals.org/).

M. Yamaura, J. Mitsushita, and S. Furuta contributed equally to this work.

Requests for reprints: Tohru Kamata, Department of Molecular Biology and Biochemistry, Shinshu University Graduate School of Medicine, 3-1-1 Asahi, Matsumoto, Nagano 390-8621 Japan. Phone: 81-263-37-2601; Fax: 81-263-37-2604; E-mail: kamatat@shinshu-u.ac.jp.

doi:10.1158/0008-5472.CAN-08-3745

provides evidence of the involvement of Nox enzymes in cell cycle control.

Materials and Methods

Cell culture and materials. A variety of human melanoma cell lines were obtained from different sources (see Supplementary Table S1) and maintained in DMEM supplemented with 10% fetal bovine serum (FBS). A human epidermal melanocyte cell line was obtained from Cascade Biologics and maintained in Medium 254 (Cascade Biologics) with HMGS (Cascade Biologics). Propidium iodide, 6-hydroxy-2, 5, 7,8-tetramethylchroman-2-carboxylic acid (a water-soluble vitamine E analogue), rabbit anticatalase antibodies, and monoclonal anti-$p21^{WAF1/C2P1}$ antibodies were purchased from Sigma; PDTC, diphenyleneiodonium (DPI), and rabbit anti-phospho CDK1 (tyr-15) antibodies from Calbiochem; and AEC substrate chromagen and horseradish peroxidase (HRP)-conjugated anti-rabbit IgG antibodies from DAKO. Rabbit anti-cdc25c antibodies were purchased from Cell Signaling and rabbit anti-p53 (FL-393) and rabbit anti–14-3-3 antibodies from Santa Cruz. Human Nox4 cDNAs were subcloned into pEGFP-C1 vectors (Clontech) containing Green Fluorescent Protein (GFP-hNox4).

Transfection and siRNA constructions. Transfection was carried out by using Lipofectamine 2000 (Invitrogen) according to the manufacturer's protocol. DNA oligonucleotides encoding siRNA with loop sequence (TTCAAGAGA) were subcloned into the H1 promoter vector, pSilencer hygro (Ambion). Nox4 siRNAs were designed as follows: 5′-CAGAA-CATTCCATATTAC-3′ for siNox4-1 and 5′-ACTTTGTTGAACTGAATG-3′ for siNox4-2, respectively. All of the constructs were verified by sequencing. A scrambled siRNA plasmid (Ambion) encodes hairpin siRNA whose sequence is not found in the human genome databases.

Isolation of stable transfectants. pSilencer vectors carrying siNox4-1, siNox4-2, and scrambled siRNA (1 μg) were transfected into MM-BP cells (10^6). Transfected cells were subjected to selection in DMEM supplemented with 10% FBS and 400 μg/mL hygromycin for 2 wk. Isolated colonies were maintained in the presence of 100 μg/mL hygromycin. The presence of stably transfected vectors in the cells was confirmed by PCR using vector-specific primers. We referred to the two cell lines carrying pSilencer siNox4-1 as siRNA1-a and siRNA1-b, a cell line carrying pSilencer siNox4-2 as siRNA2, and a cell line carrying pSilencer scrambled siRNA as scrambled.

Reverse transcription-PCR and real-time PCR. Total RNAs (5 μg) were extracted from cells with TRIzol (Invitrogen) and reverse-transcribed by Power Script (Clonetech) with Oligo dT primers (Invitrogen). The resultant cDNA was PCR amplified for human NOX1-5 by using human sense and antisense primers:

sense 5′-GGAGCAGGAATTGGGGTCAC-3′ and antisense 5′-TTGCTGTCCCATCCGGTGAG-3′ for Nox1; sense 5′-GGAGTTTCAAGATGCGTGGAAACTA-3′ and antisense 5′-GCCAGACTCAGAGTTGGAGATGCT-3′ for Nox2; sense 5′-GGATCGGAGTCACTCCCTTCGCTG-3′ and antisense 5′-ATGAACACCTCTGGGGTCAGCTGA-3′ for Nox3; sense 5′-CTCAGCGGAATCAATCAGCTGTG-3′ and antisense 5′-AGAGGAACACGACAATCAGCCTTAG-3′ for Nox4; sense 5′-ATCAAGCGGCCCCCTTTTTTTCAC-3′ and antisense 5′-CTCATTGTCACACTCCTCGACAGC-3′ for Nox5

Nox4 expression in various melanoma cell lines was evaluated with real-time PCR (35 cycles) using Taqman Gene Expression assay (Applied Biosystems) with glyceraldehyde-3-phosphate dehydrogenase as an internal control.

Growth curve. Cells (10^4) were grown in the presence or absence of antioxidants and DPI, and the numbers of live cells were determined by trypan blue exclusion. Alternatively, cells were inoculated and labeled with [^{3}H] thymidine (0.1 μCi; GE Healthcare) in the presence or absence of the above chemicals. Labeled cells were precipitated with 10% chilled trichloroacetic acid for 10 min, and the incorporated radioactivity was determined by nitrocellulose filtration, followed by scintillation counting.

Soft agar assay. The assay was performed as described previously (4). The appearance of colonies was monitored for up to 12 d. The numbers of colonies larger than 4 mm were counted.

Immunoblotting. Cells were lysed in radioimmunoprecipitation assay buffer [PBS, 0.1% SDS, 1% Na-deoxycholate, 1% Triton X-100, 50 mmol/L NaF, 1 mmol/L sodium orthovanadate, 10 mmol/L sodium PPi leupeptin (10 μg/mL), pepstatin A (10 μg/mL), and phenylmethylsulfonyl fluoride (1 mmol/L)]. Extracted proteins were separated by SDS-PAGE and subjected to immunoblotting with indicated antibodies.

Tumorigenecity analysis. To determine tumor formation by each transfected cell line, trypsinized cells (10^7) were suspended in 0.2 mL of PBS, and the cell suspensions were inoculated s.c. into athymic mice. All of the animals were observed for the formation of tumors for up to 3 wk. The size of tumor was measured at the 12th day with an external caliper, and volume was calculated.

Preparation of anti-Nox4 antibodies. The COOH-end peptides of Nox4 (CLSNQNNSYGTRFFYNKESFS) cross-linked to keyhole limpet hemocyanin

Table 1. A summary of histochemical study

Patient	Age	Sex	Primary lesion	Sample	Clinical type	Nox4 expression
1	69	M	Foot	Primary	ALM	Positive
2	83	M	Finger	Primary	ALM	Negative
3	69	F	Foot	Primary	ALM	Positive
4	61	F	Foot	Primary	ALM	Negative
5	76	M	Finger	Primary	ALM	Negative
6	68	F	Lower leg	Primary	SSM	Positive
7	48	F	Rt. arm	LN meta	SSM	Negative
8	76	M	Head	LN meta	SSM	Negative
9	67	M	Upper back	Primary	SSM	Positive
10	85	M	Neck	Primary	SSM	Negative
11	64	F	Lower leg	Primary	SSM	Negative
12	53	F	Abdomen	Primary	NM	Negative
13	63	F	Genital Mucosa	LN meta	mucosal	Negative

NOTE: Melanoma tissues isolated from patients were processed for immunohistochemistry using anti-Nox4 antibodies as described in Materials and Methods.

Abbreviations: ALM, acral lentiginous melanoma; rt. arm, right arm; LN, lymphnode; SSM, superficial spreading melanoma; NM, nodular melanoma.

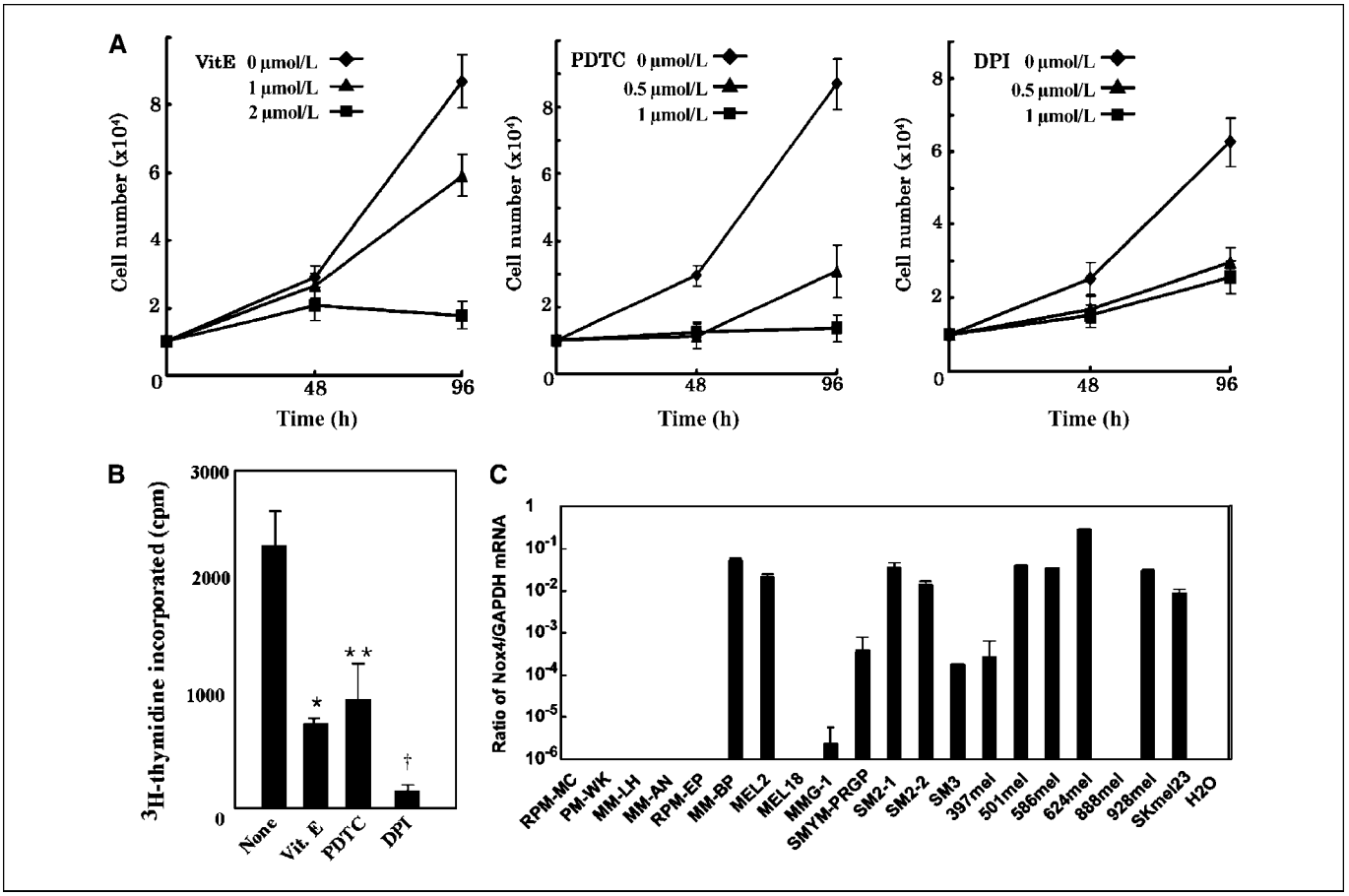

Figure 1. Effect of antioxidants and DPI on MM-BP cell growth and Nox4 expression in melanoma cell lines. *A,* cells were cultured in the presence or absence of vitamine E, PDTC, and DPI until live cells were harvested at the indicated times and the number of live cells was determined. *Points,* mean in triplicated dishes; *bars,* SD. *B,* alternatively, MM-BP cells (10^5) were metabolically labeled with [^{3}H]thymidine for 48 h in the presence of 2 μmol/L vitamine E, 1 μmol/L PDTC, or 1 μmol/L DPI. The radioactivity incorporated were determined. *Columns,* mean (n = 4); *bars,* SD. P^*, P^{**}, and $P^+ < 0.05$ versus none. *C,* The levels of Nox4 expression in various melanoma cell lines were examined by real-time PCR. *Columns,* mean of duplicated assays; *bars,* SD.

were immunized into rabbits, and the antiserum was affinity purified. In some experiments, mouse monoclonal antibodies against Nox4 (gift by Dr. B. Goldstein, Department of Medicine, Jefferson Medical College, Thomas Jefferson University, Philadelphia, PA) were used.

Measurement of intracellular ROS. Forty-eight hours after plating, cells were incubated with HBSS (Invitrogen) containing 10 μmol/L 2;7′-dichlorodihydrofluorescein diacetate (Molecular Probes) for 10 min at 37°C. Images were obtained with a Zeiss confocal microscope. Fluorescence was quantitated on an arbitrary unit and the data represent the fluorescence intensity of ~50 random cells obtained from three separate fields.

Determination of the cellular DNA content by fluorescence-activated cell sorting analysis. MM-BP cells were plated at 1×10^5 cell density per 60-mm dish, starved for 48 h in DMEM containing 0.5% serum, and then maintained for 48 h in DMEM containing 10% serum. Trypsinized cells (10^6–10^7) were subjected to cell cycle analysis using propidium iodide as described (18). Relative DNA content of nuclei was measured by a fluorescence-activated cell sorter (Becton Dickinson).

Immunohistochemistry. Primary or metastatic melanoma tissues were obtained from informed patients. Immunohistochemistry was performed on 4-μm thick formalin-fixed paraffin-embedded tissue. Paraffin sections were dewaxed in xylene and rehydrated with distilled water. The tissue sections were activated in Tris-EDTA buffer (pH 9) in the microwave oven for 25 min. The slides were subsequently incubated with the purified rabbit anti-human Nox4 antibody, followed by HRP-conjugated anti-rabbit IgG antibodies. For controls, the antibodies preadsorbed with Nox4 peptide antigens were used. Staining was visualized with AEC substrate chromogen, followed by hematoxylin counterstaining. Indirect immunofluorescence staining was performed and samples were observed under a confocal microscope (LSM510; Carl Zeiss) as described previously (8).

Statistical analysis. The statistical analysis was performed with Student's t test. For multiple treatment groups, a factorial ANOVA followed by Bonferroni's t test was applied. Differences with P values of <0.05 were considered to be statistically significant.

Results

Effects of antioxidants and DPI on melanoma cell growth. To explore the functional role of ROS-generating enzymes in malignant melanoma, we first examined whether proliferation of melanoma cells requires ROS production. Human melanoma MM-BP cells (19) were treated with increasing amounts of a dietary antioxidant vitamine E and a thiol-containing antioxidant pyrrolidine dithiocarbamate (PDTC). Consistent with other reports (15), vitamine E decreased the growth of MM-BP cells in liquid culture (Fig. 1*A*) and PDTC was also effective in inhibiting the cell growth (Fig. 1*A*). Furthermore, DPI, a flavoprotein-dependent oxidase inhibitor, showed the growth inhibitory effect (Fig. 1*A*), whereas rotenone, a mitochondrial oxidase inhibitor, had little or no effect (data not shown). The inhibitory effects of vitamine E, PDTC, and DPI were also confirmed by cell proliferation assay using [^{3}H] thymidine incorporation (Fig. 1*B*). These results suggest that Nox

family enzymes participate in growth control involving ROS in MM-BP cells. To further study the source of ROS generation, we examined the expression of Nox family mRNAs in MM-BP cells. Reverse transcription-PCR analysis revealed that a relatively high amount of Nox4 mRNA was expressed in MM-BP cells compared with other Nox family homologues including Nox1, Nox2, Nox3, and Nox5 (Fig. 2*A*). No appreciable Nox4 messages were detected in melanocytes under the condition used (Fig. 2*A*). In addition, real-time PCR showed that significant levels of Nox4mRNA were expressed in 13 of 20 melanoma cell lines with different origins (Supplementary Table S1; Fig. 1*C*). Accordingly, it is conceivable that up-regulation of Nox4 is not a particular characteristics of MM-BP cells but a frequent event among melanoma cell lines. In the subsequent study, we therefore focused on the Nox4 action in MM-BP cells.

Nox4 is involved in ROS generation in melanoma cells. To probe the functional role of Nox4 in melanoma, we stably transfected the expression vectors carrying siRNAs for Nox4 into MM-BP cells. With the isolated clones, RT-PCR and immunoblotting analysis showed that loading with siRNA1 or siRNA2 significantly decreased the amounts of Nox4 mRNAs (Fig. 2*A*) and Nox4 proteins (the data for a cell line, siRNA1-b, are not shown; Fig. 2*A*) compared with those in the scrambled siRNA preparation, which indicated that introduced Nox4 siRNAs effectively repressed the Nox4 expression. To test whether Nox4 mediates intracellular ROS production, generation of H_2O_2, a dismutated metabolite of Nox4-derived superoxide was measured in Nox4siRNA-transfected cell lines after addition of the fluorescent oxidant indicator dye 2;7′-dichlorodihydrofluorescein diacetate. Although intracellular DCF fluorescence was detected in scrambled siRNA-transfected MM-BP cells, this fluorescence was sharply attenuated in siRNA1-a, siRNA1-b, and siRNA2 cells (Supplementary Fig. S1; Fig. 2*B*). The results indicate that Nox4 siRNAs inhibit spontaneous oxidant generation in MM-BP cells, suggesting the involvement of Nox4 in ROS production in melanoma cells.

Effects of Nox4 siRNAs on melanoma proliferation. Because DPI or antioxidants treatment blocked proliferation of MM-BP cells (Fig. 1*A–D*), we next examined whether suppression of the Nox4 activity by Nox4siRNAs induces dysregulation of cell proliferation. Soft agar assay as an *ex vivo* model of tumorigenicity shows

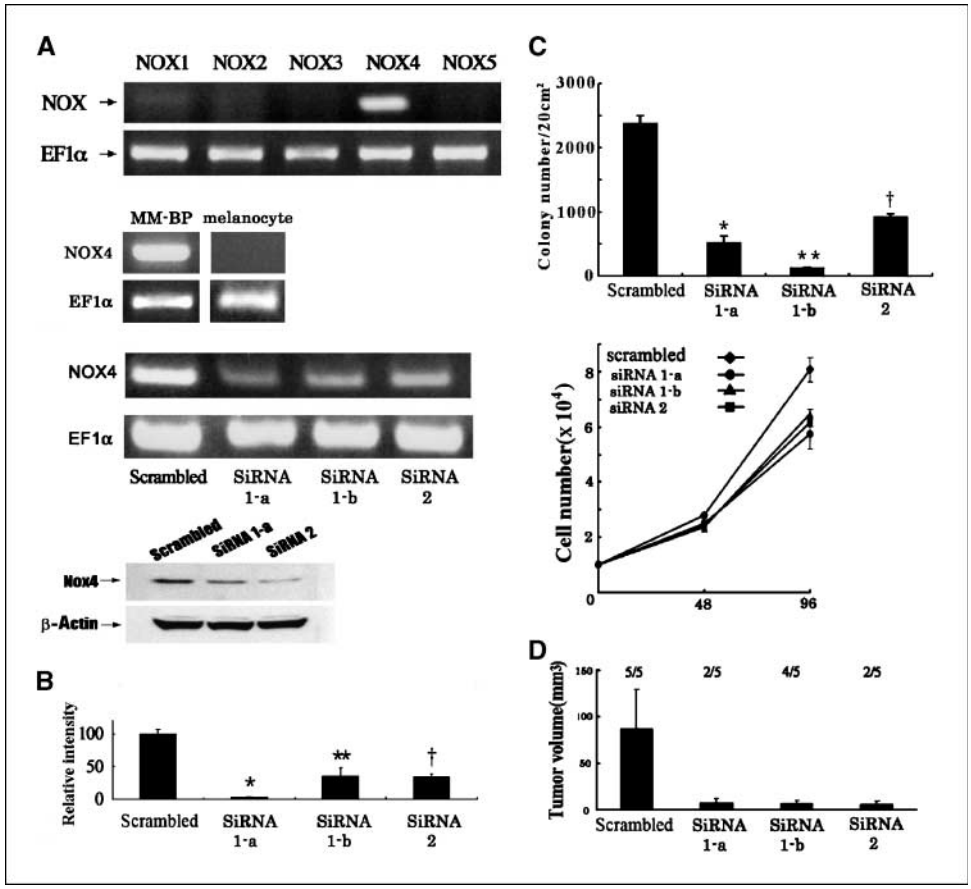

Figure 2. mRNA expression of Nox family members in MM-BP cells and suppression of Nox4 expression by Nox4 siRNAs. *A,* total RNAs were extracted from MM-BP cells and mRNA expressions of Nox isoforms were analyzed by RT-PCR with EFIα expression as internal controls (*top*). RT-PCR was performed with melanocyte and MM-BP cells. Total RNAs were extracted from the cell lines carrying scrambled siRNA or Nox4-specific siRNAs (*1-a, 1-b*, or *2*) and RT-PCR, with EF1αmRNA as a control, was performed to analyze Nox4 mRNA expression (*middle*). Alternatively, lysates (10^6 cells) prepared from these cell lines were subjected to immunoblotting with mouse monoclonal anti-Nox4 antibodies (*top*) or anti-βactin antibodies (*bottom*). *B,* Nox4siRNAs inhibit production of ROS in MM-BP cells. The cell lines (10^7cells) carrying Nox4siRNAs or scrambled siRNA were loaded with 2;7'-dichlorodihydrofluorescein diacetate for 10 min. ROS generation was detected by a confocal microscope. *Columns,* mean of three separate experiments (arbitrary unit); *bars,* SD. P^*, P^{**}, and $P^+ < 0.05$ versus scrambled. *C,* anchorage-independent cell growth on soft agar (*top*). The cell lines were seeded in soft agar and colonies were scored. *Columns,* mean of separate experiments ($n = 3$); *bars,* SD. P^*, P^{**}, and $P^+ < 0.05$ versus scrambled. Cell proliferation in liquid culture (*bottom*). The cell numbers were determined at the indicated time points. *Points,* mean of three separate experiments; *bars,* SD. *D,* tumor formation by cell lines carrying Nox4 siRNAs. Each cell lines were injected into nude mice, and tumor volume was measured; *columns,* mean; *bars,* SD. Fraction numbers show the ratio of the mice bearing tumors to the total mice used.

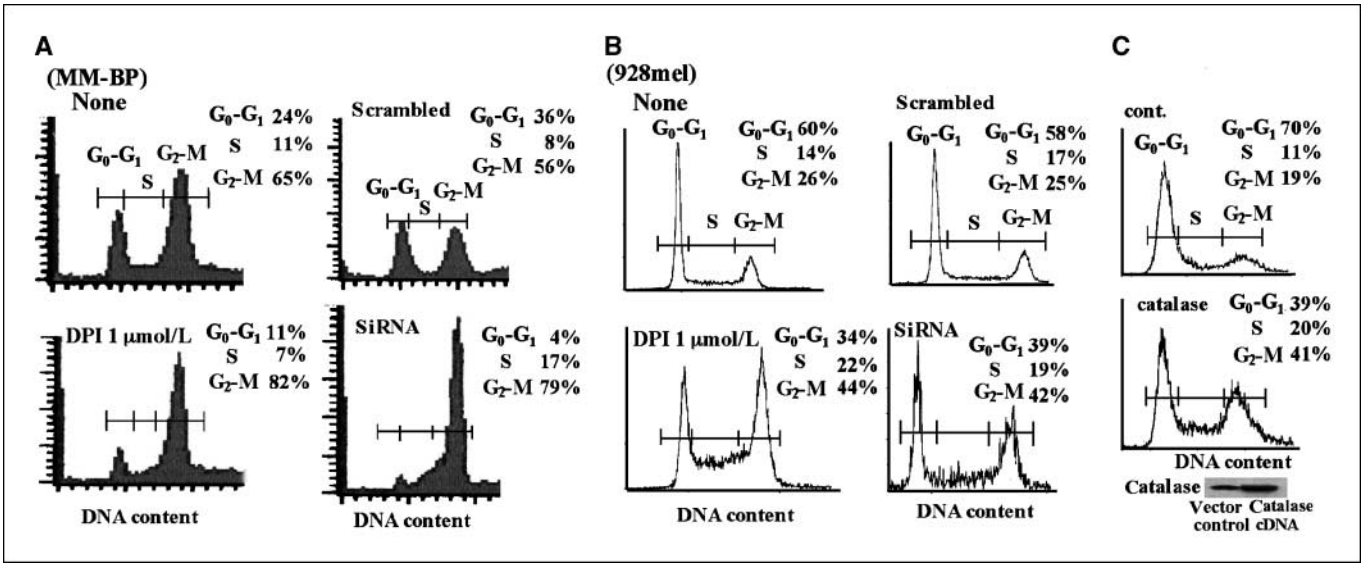

Figure 3. Cell-cycle perturbation by DPI, siNox4 RNAs, and catalase. *A,* parental MM-BP cells were serum-starved for 48 h and treated with or without 2 μmol/L DPI for 24 h (*left*). Alternatively, the cell lines carrying Nox4siRNAs or scrambled siRNAs were serum-starved for 48 h (*right*). Cells were then refed with the growth medium for 72 h and subjected to flow cytometric analysis. The proportion of nuclei in each pair of the cell cycle is shown. Similar results were obtained in three separate experiments. *B,* 928mel cells were serum starved, treated with or without DPI as in *A* (*left*). Alternatively, 928mel cells were transiently transfected with Nox4siRNAs or scrambled siRNAs and serum starved (*right*). Cells were then refed with the growth medium for 72 h and subjected to flow cytometric analysis. Similar results were obtained in three separate experiments. *C,* transfection of catalase increases G_2-M cell cycle arrest. MM-BP cells (10^5) were transfected with 5 μg of control vectors or pS-CAT (*catalase*), serum-starved for 48 h, and refed with the growth medium for 48 h. Cells were then analyzed for DNA content by flow cytometry. Similar results were obtained in three separate experiments. Expression of transfected catalase was determined by immunoblotting (*IB*) with anticatalase antibodies. *IP,* immunoprecipitation.

that Nox4siRNAs caused a significant reduction in anchorage-independent growth of MM-BP cells compared with that caused by scrambled siRNAs (Fig. 2*C*). The inhibitory effect of Nox4siRNAs on cell growth was detected in liquid culture, as well (Fig. 2*C*). These data indicate that Nox4-generated ROS are required to sustain growth of melanoma cells.

Suppression of tumor formation by Nox4siRNAs. Inhibition of anchorage-independent growth of MM-BP cells by Nox4siRNAs (Fig. 2*C*) suggests that silencing of Nox4 by Nox4siRNAs suppresses transformation phenotype of the cells. To test whether MM-BP cells become less tumorigenic through overexpression of Nox4siRNAs, the cells transfected with either scrambled or Nox4siRNAs were implanted into athymic nude mice. Although scrambled siRNA-transfected cells formed significant tumors in 2 weeks, introduction of Nox4siRNAs markedly decreased tumor growth (Fig. 2*D*). Thus, the results indicate that Nox4siRNAs inhibit tumorigenicity of MM-BP cells, suggesting the critical mediating role of Nox4-derived ROS in development of some types of melanomas.

Because tumor progression is often associated with augmented cell motility and invasiveness of cancer cells, we compared scrambled siRNA-transfected cells with Nox4siRNA-transfected cells for the cell migration activity by Matrigel assay, but the migration was not suppressed by inhibition of Nox4 (Supplementary Fig. S3), implying that Nox4 is not involved in the regulation of the motility of MM-BP cells.

Inhibition of Nox4 induces cell cycle arrest. To further analyze the mechanism underlying Nox4siRNA-induced growth inhibition, cell cycle distribution of MM-BP cells was analyzed by flow cytometry. Cells were serum starved for 48 h to arrest their growth and refed with the growth medium in the presence or absence of DPI. Of note, treatment of MM-BP cells with DPI for 24 hours was found to induce an accumulation of cells in G_2-M phase (Fig. 3*A*). A marked increase of cell population in G_2-M phase was also observed with the cell line, siRNA1-a (Fig. 3*A*). Similarly, another Nox4-positive melanoma cell line, 928mel (Table 1) displayed cell accumulation in G_2-M phase when treated with DPI or transiently transfected with Nox4siRNAs (Fig. 3*B*). Furthermore, depletion of hydrogen peroxide by overexpression of catalase in MM-BP cells resulted in G_2-M cell cycle arrest (Fig. 3*C*), which is consistent with the notion that Nox4-derived ROS mediate cell cycle progression from G_2-M phase.

To characterize the molecular machinery involved in G_2-M cell cycle arrest upon ablation of Nox4, the expression of some of cell cycle–controlling genes was examined. A protein kinase CDK1 (cdc2) plays an important role in the regulation of the G_2-M cell cycle phase. Activation of CDK1 (dephosphorylation at Tyr-15) is required for transition from the G_2-M phase, whereas its inactivation (phosphorylation at Tyr-15) causes G_2-M cell cycle block (20). We therefore examined the phosphorylation state of the Tyr-15 of CDK1 by immunoblotting with anti-phospho CDK1 (Tyr-15) antibodies. The level of Tyr-15 phosphorylation was increased in MM-BP cells 24 hours after exposure to DPI (Fig. 4*A*), which chronologically coincided with induction of G_2-M phase cell cycle arrest by DPI treatment. Moreover, introduction of Nox4siRNAs into MM-BP cells resulted in a similar increase in Tyr-15 phosphorylation of CDK1 compared with that in scrambled siRNA-transfected cells (Fig. 4*A*). The total amount of CDK1 proteins was not changed (data not shown). Likewise, Tyr-15 phosphorylation of CDK1 was induced in DPI-treated or Nox4siRNA-transfected melanoma 928mel cells (Fig. 4*A*). These data suggest that the G_2-M cell cycle arrest was induced as CDK1 was inactivated. p53 and $p21^{WAF1/CIP1}$, such as CDK1, have been reported to regulate the G_2-M transition and be critical in sustaining the G_2-M cell cycle arrest after DNA damage through inhibition of CDK1 (21, 22). DPI treatment had no

appreciable effect on either p53 or $p21^{WAF1/CIP1}$ protein levels in MM-BP cells for at least 24 hours, as determined by immunoblotting analysis (Fig. 4*B*). These results suggest that induction of G_2-M arrest by Nox4 inhibition is controlled by a mechanism independent of both p53 and $p21^{WAF1/CIP1}$.

It has been known that the activity of CDK1 is regulated by cdc25c phosphatase through dephosphorylation of the Tyr-15 residue, and that the activity of cdc25c is modulated by phosphorylation. To determine whether phosphorylation of cdc25c was regulated by Nox4, we analyzed fractions of cdc25c mobility by immunoblotting. Consistent with the previous report (23), the unphosphorylated form "a" and phosphorylated form "b" (Ser216 phosphorylation) of cdc25c were detected in untreated MM-BP cells (Fig. 4*C*). In contrast, addition of DPI for 24 hours induced hyperphosphorylation of cdc25c, which is indicated by the appearance of a slower-migrated form "c" of cdc25c (refs. 23, 24; Fig. 4*C*). Similarly, the level of the hyperphosphorylated cdc25c protein was elevated in a Nox4siRNA-transfected MM-BP cell line, whereas it was not increased in scrambled siRNA-transfected cells (Fig. 4*C*). Hyperphosphorylation of cdc25c is thought to prolong its remaining in the cytoplasm due to increased binding with 14-3-3 proteins, inhibiting the interaction between cdc25c and CDK1 in the nucleus (19, 25). Indeed, immunostaining showed that exclusion of cdc25c from the nuclei was increased in both DPI-exposed and Nox4siRNA-transfected MM-BP cells (Fig. 4*D*). Coprecipitation studies showed that Nox4siRNA transfection resulted in enhanced binding of cdc25c with 14-3-3 when compared with scrambled siRNAs transfection (Fig. 4*D*). Thus, these data suggest that hyperphosphorylation of cdc25c mediates both DPI and Nox4siRNA-induced Tyr-15 phosphorylation of CDK1, leading to cell cycle arrest at G_2-M stage.

The growth inhibition is frequently accompanied by induction of apoptosis. By using terminal deoxynucleotidyl-transferase–mediated dUTP nick-end labeling assay, we therefore examined whether or not suppression of the Nox4 activity induces apoptosis. No significant changes in cell survival rate were detected after DPI or Nox4siRNA treatment (Supplementary Fig. S4), which is consistent with the flow cytometric profiles without any sub-G_1 peak representing apoptotic cell population (Fig. 3*A* and *B*). From these data, we conclude that the observed growth inhibitory effects of DPI and Nox4siRNAs in both soft agar and liquid culture are due to cell cycle arrest at G_2-M transition rather than apoptosis.

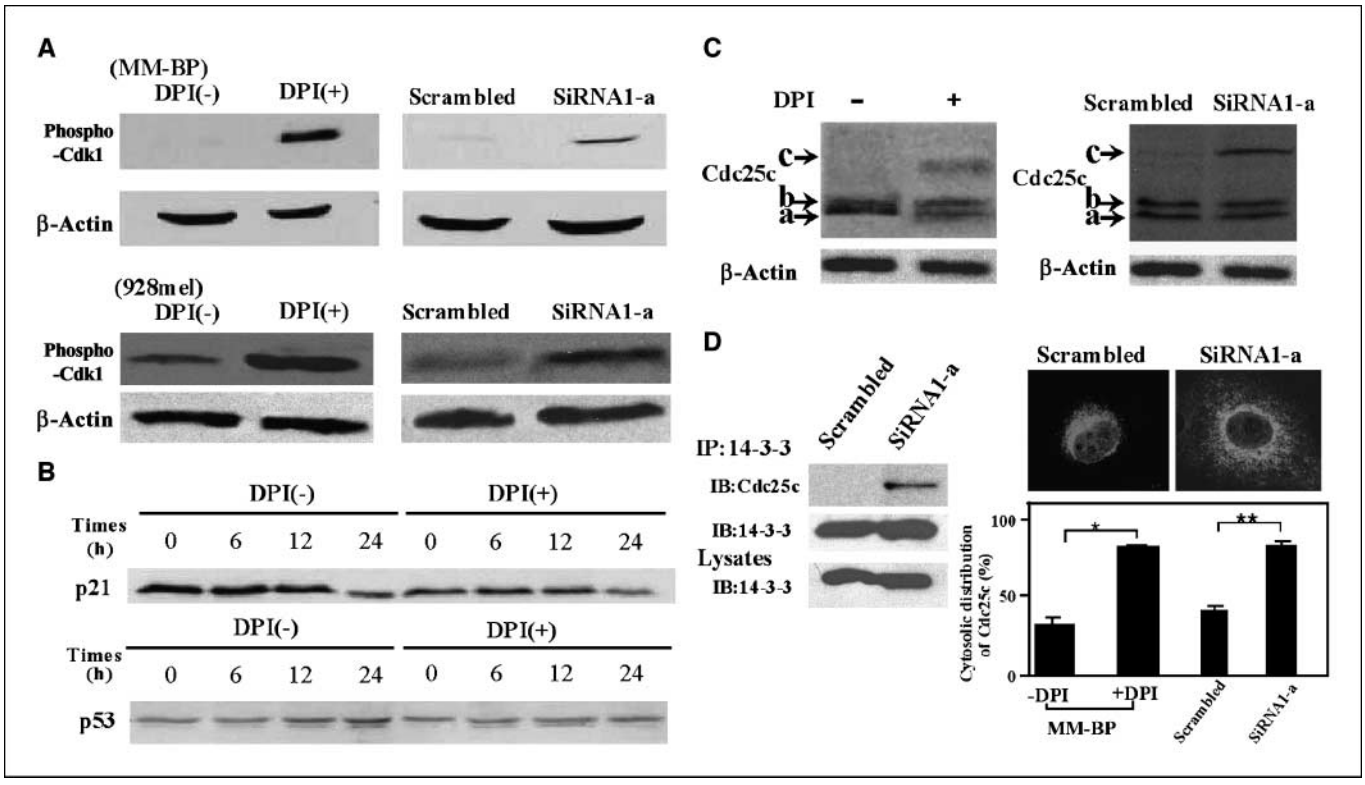

Figure 4. Effects of DPI and Nox4 siRNAs on G_2-M phase cell cycle controlling proteins. *A,* MM-BP cells were serum-starved, treated with or without DPI (2 μmol/L), and refed in growth media as in Fig. 3*A*. Alternatively, the cell line siRNA1-a or scrambled was serum-starved and refed in growth media as above. Then, cell lysates were subjected to immunoblotting with anti-phospho CDK1 (tyr-15) antibodies (*top*). 928mel cells were serum starved for 48 h, treated with or without DPI (2 μmol/L) for 24 h, and refed in growth media for 72 h. Alternatively, 928mel cells transiently transfected with Nox4siRNAs or scrambled siRNAs were serum starved and refed with growth media as above. Lysates were subjected to immunoblotting using anti-phospho (Tyr-15) CDK1 antibodies (*bottom*). *B,* MM-BP cells were incubated with or without DPI (2 μmol/L) for the indicated time periods. Cell lysates were processed for immunoblotting using antibodies to $p21^{WAF1/CIP1}$ or p53. *C,* DPI or Nox4siRNA-induced hyperphosphorylation of cdc25c. MM-BP cells were serum starved for 48 h and treated with 2 μmol/L DPI for 15 h. Alternatively, cell lines, siRNA1-a or scrambled were serum starved for 48 h and refed with the growth medium. Lysates were subjected to immunoblotting with anti-cdc25c antibodies. Note that form a and b bands partially overlapped due to overloading samples. Protein loading was monitored by β-actin. *D,* MM-BP cells were treated with or without DPI as in *A*. Cell lines, scrambled and siRNA1-a were serum starved and refed with complete growth medium for 24 h as in *A*. Cells were fixed and stained with rabbit anti-cdc25c antibodies and CY-3–conjugated anti-rabbit IgG antibodies (Molecular Probes). *Right,* immunostained patterns. Histograms show means ± SD of 3 separate experiment (average number of counted cells is 80). $P < 0.05$ (*) and $P < 0.05$ (**) versus DPI (−) and scrambled, respectively. After serum starvation/refeeding, lysates prepared from scrambled or siRNA 1-a cells were immunoprecipitated with anti–14-3-3 antibodies, followed by immunoblotting with anti-cdc25c antibodies (*left*). 14-3-3 proteins in lysates and immunoprecipitates were identified by immunoblotting with 14-3-3 antibodies.

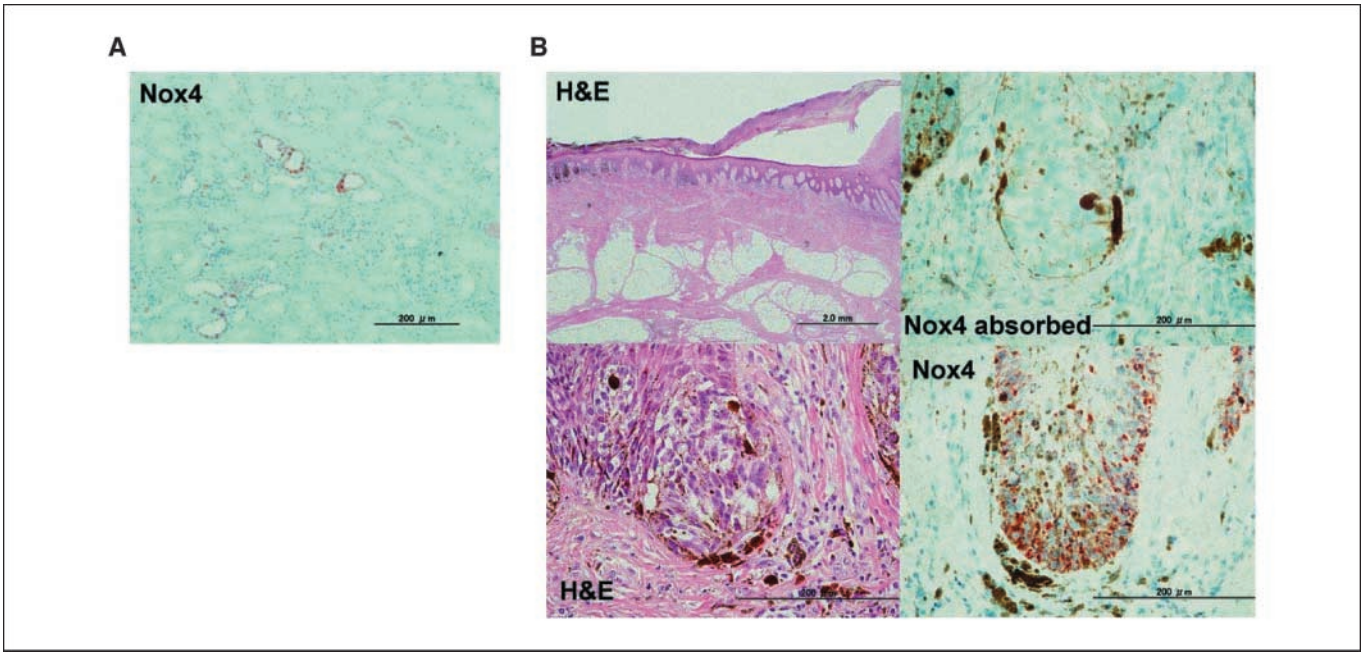

Figure 5. Expression of Nox4 in melanoma tissues. Biopsy specimens of melanoma were surgically isolated and immunohistochemistry with rabbit anti-Nox4 antibodies were performed. Nox4-positive melanoma cells were found in the epidermal nest (*B, Nox4*). Immunoadsorption of the antibodies with the Nox4 peptide antigen abolished Nox4 staining (*B, Nox4 adsorbed*). In control experiments (*A*), the antibodies detected Nox4 expression in normal renal cortex as reported (26). Tissues were counterstained with hematoxylin.

Expression of Nox4 in melanoma tissues. To examine whether Nox4 expression is really up-regulated in melanoma tissues, Nox4 expression patterns were evaluated in 13 primary or metastatic melanoma samples isolated from patients by immunohistochemistry using antibodies against Nox4. Immunoblotting analysis showed that the raised Nox4 antibodies recognize Nox4 proteins (Supplementary Fig. S2). The result was then confirmed by showing the staining of the proximal renal tubles of normal kidney with the antibodies as reported earlier (Fig. 5*A*; ref. 26). Nox4 was expressed in 4 of 13 melanoma tissues, including 5 acral melanomas, 6 superficial spending melanomas, 1 nodular melanoma, and 1 mucosal melanoma (Table 1). Of these, two acral melanomas and two superficial spending melanomas expressed Nox4. Frequency of Nox4 expression seemed independent of clinical type. Interestingly, Nox4 was strongly expressed in the nests in epidermis (Fig. 5*B*) but less in the metastatic lymph nodes. In all of the Nox4-positive melanoma tissues, Nox4 was localized in the cytoplasm or perinucleus. Immunoabsorption of the antibodies with the Nox4 peptide antigen abolished most of the staining, indicating that the staining is Nox4 specific (Fig. 5*B*). No Nox4 expression was observed in normal skin tissues and cultured melanocytes (data not shown). These observations show that Nox4 is expressed not only in cultured melanoma cell lines but indeed in melanoma tissues, which lends additional support to the view that Nox4 plays some important role in pathogenesis of melanoma.

Discussion

Malignant melanoma is the most aggressive form of skin cancer. ROS production has been partly implicated in the development of melanoma and its resistance to radiation and chemotherapy, but the functional roles of ROS are not fully understood. Here, we show that superoxide generation by Nox4 is required for proliferation of melanoma MM-BP cells and formation of tumors derived from MM-BP cells in athymic mice, suggesting a critical role for Nox4 in maintenance of malignant transformation phenotype of melanoma. Furthermore, our studies reveal that Nox4 mediates cell proliferation by regulating G_2-M cell cycle progression because inhibition of Nox4 activity by either Nox4-specific siRNAs or DPI caused G_2-M cell cycle arrest. This is also supported by the facts that G_2-M arrest upon Nox4 inhibition was observed in another melanoma cell line, 928mel, and that G_2-M block was induced by catalase-mediated depletion of hydrogen peroxide, a dismutated metabolite of Nox4-generated superoxide. To our knowledge, this is the first observation that Nox enzyme–mediated signalings link to the cell cycle controlling events.

CDK1 (cdc2) kinase that interacts with cyclin B is a key mitosis-promoting kinase in the control of the G_2-M cell cycle progression. Namely, activation of CDK1, complexed with cyclin B, promotes transition from G_2 to M phase of the cell cycle. CDK1 is activated by cdc25c phosphatase that dephosphorylates CDK1 at Tyr-15 residues. Our data indicate that both Nox4siRNAs and DPI treatment inactivate cdc25c, causing increased phosphorylation of CDK1 on Tyr-15, a hallmark of the G_2-M checkpoint. The activity of cdc25c is believed to be inactivated mainly by two mechanisms: (*a*) phosphorylation of cdc25c at Thr-47 decreases its phosphatase activity; (*b*) hyperphosphorylation of cdc25c creates a binding site for 14-3-3 proteins, which sequester cdc25c to the cytoplasm and thereby interfere with its interaction with CDK1 in the nucleus (19, 25). As abrogation of Nox4-generated ROS led to induction of hyperphosphorylated cdc25c, the most-likely possibility is that the G_2-M cell cycle arrest was caused via the second mechanism. Although p53 and $p21^{WAF1/C2P1}$ have also been implicated in regulation of the G_2-M cell cycle arrest after DNA damage through inhibition of CDK1 (21, 22), the expression levels of p53 and $p21^{WAF1/C2P1}$ were unaffected by suppression of the Nox4 activity

(Fig. 4*B*), rendering their involvement unlikely. The elevated expression of cyclin D and CDK4, critical gatekeepers at the G_1-S check point and targets to the Ras-B-Raf pathway, is frequently found in melanoma (27, 28). The dysfunction of these cell cycle controlling genes is considered to result in abnormal proliferation of melanoma cells (29). Thus, our observation would be significant in the sense that it revealed an alternative deregulation of melanoma cell growth depending on the aberrant control of a G_2-M checkpoint. It will be of interest in future studies to identify a molecule(s) mediating a signal transmission from Nox4-generated ROS to cdc25c-CDK1 connection.

Immunohistochemical experiments revealed that Nox4 expression was increased in tissues obtained from several types of melanoma biopsies, whereas no expression of Nox4 was detected in normal tissues adjacent to the tumor. Evidence indicates that expression of Nox4 is augmented not only in human melanoma cell lines but indeed occurs during *in vivo* melanoma development. Notably, melanoma in epidermis contains a high level of Nox4, but metastatic melanoma in lymph nodes exhibits a decrease in the Nox4 level. Elevated ROS production by up-regulated Nox enzymes may increase a risk of cancer in early stages by causing persistent proinflammatory responses (30). At least, Nox4 does not seem to contribute to the motile activity of melanoma cells, which is related to invasiveness of tumors (see Result).

Overall, our study showed the functional requirement of Nox4-generated ROS for transformation phenotype associated with melanoma and revealed a novel cell cycle regulation effect of Nox4 in melanoma cells. The discovery has significant implications in understanding the molecular mechanism of melanocyte tumor development and Nox4 could be a potential molecular target in the treatment of melanoma.

Disclosure of Potential Conflicts of Interest

No potential conflicts of interest were disclosed.

Acknowledgments

Received 10/1/2008; revised 12/1/2008; accepted 12/29/2008; published OnlineFirst 3/10/09.

Grant support: Grant on Cancer Research in Applied Areas from the Ministry of Science and Culture of Japan (T. Kamata).

The costs of publication of this article were defrayed in part by the payment of page charges. This article must therefore be hereby marked *advertisement* in accordance with 18 U.S.C. Section 1734 solely to indicate this fact.

We thank Dr. T. Finkel for catalase plasmid and technical assistance for M. Ito and PY. Zhang, Dr. N. Colburn for a critical reading of the manuscript and, F. Ushiyama for typing the manuscript.

References

1. Lambeth JD. NOX enzymes and the biology of reactive oxygen. Nat Rev Immunol 2004;4:181–9.
2. Lassegue B, Sorescu D, Szocs K, et al. Novel gp91(phox) homologues in vascular smooth muscle cells: nox1 mediates angiotensin II-induced superoxide formation and redox-sensitive signaling pathways. Circ Res 2001;88:888–94.
3. Suh YA, Arnold RS, Lassegue B, et al. Cell transformation by the superoxide-generating oxidase Mox1. Nature 1999;401:79–82.
4. Mitsushita J, Lambeth JD, Kamata T. The superoxide-generating oxidase Nox1 is functionally required for Ras oncogene transformation. Cancer Res 2004;64:3580–5.
5. Pedruzzi E, Guichard C, Ollivier V, et al. NAD(P)H oxidase Nox-4 mediates 7-ketocholesterol-induced endoplasmic reticulum stress and apoptosis in human aortic smooth muscle cells. Mol Cell Biol 2004;24:10703–17.
6. Park HS, Jung HY, Park EY, Kim J, Lee WJ, Bae YS. Cutting edge: direct interaction of TLR4 with NAD(P)H oxidase 4 isozyme is essential for lipopolysaccharide-induced production of reactive oxygen species and activation of NF-κB. J Immunol 2004;173:3589–93.
7. Szatrowski TP, Nathan CF. Production of large amounts of hydrogen peroxide by human tumor cells. Cancer Res 1991;51:794–8.
8. Shinohara M, Shang WH, Kubodera M, et al. Nox1 redox signaling mediates oncogenic Ras-induced disruption of stress fibers and focal adhesions by down-regulating Rho. J Biol Chem 2007;282:17640–8.
9. Vaquero EC, Edderkaoui M, Pandol SJ, Gukovsky I, Gukovskaya AS. Reactive oxygen species produced by NAD(P)H oxidase inhibit apoptosis in pancreatic cancer cells. J Biol Chem 2004;279:34643–54.
10. Mochizuki T, Furuta S, Mitsushita J, et al. Inhibition of NADPH oxidase 4 activates apoptosis via the AKT/apoptosis signal-regulating kinase 1 pathway in pancreatic cancer PANC-1 cells. Oncogene 2006;25:3699–707.
11. Brar SS, Corbin Z, Kennedy TP, et al. NOX5 NAD(P)H oxidase regulates growth and apoptosis in DU 145 prostate cancer cells. Am J Physiol Cell Physiol 2003;285:C353–69.
12. Fu X, Beer DG, Behar J, Wands J, Lambeth D, Cao W. cAMP-response element-binding protein mediates acid-induced NADPH oxidase NOX5-S expression in Barrett esophageal adenocarcinoma cells. J Biol Chem 2006;281:20368–82.
13. Sander CS, Hamm F, Elsner P, Thiele JJ. Oxidative stress in malignant melanoma and non-melanoma skin cancer. Br J Dermatol 2003;148:913–22.
14. Church SL, Grant JW, Ridnour LA, et al. Increased manganese superoxide dismutase expression suppresses the malignant phenotype of human melanoma cells. Proc Natl Acad Sci U S A 1993;90:3113–7.
15. Prasad KN, Edwards-Prasad J. Effects of tocopherol (vitamin E) acid succinate on morphological alterations and growth inhibition in melanoma cells in culture. Cancer Res 1982;42:550–5.
16. Valencia A, Kochevar IE. Nox1-based NADPH oxidase is the major source of UVA-induced reactive oxygen species in human keratinocytes. J Invest Dermatol 2008;128:214–22.
17. Brar SS, Kennedy TP, Sturrock AB, et al. An NAD(P)H oxidase regulates growth and transcription in melanoma cells. Am J Physiol Cell Physiol 2002;282:C1212–24.
18. Byers HR, Etoh T, Doherty JR, Sober AJ, Mihm MC, Jr. Cell migration and actin organization in cultured human primary, recurrent cutaneous and metastatic melanoma. Time-lapse and image analysis. Am J Pathol 1991;139:423–35.
19. Lee MS, Ogg S, Xu M, et al. cdc25+ encodes a protein phosphatase that dephosphorylates p34cdc2. Mol Biol Cell 1992;3:73–84.
20. Harper JW, Adami GR, Wei N, Keyomarsi K, Elledge SJ. The p21 Cdk-interacting protein Cip1 is a potent inhibitor of G1 cyclin-dependent kinases. Cell 1993;75:805–16.
21. Xiong Y, Hannon GJ, Zhang H, Casso D, Kobayashi R, Beach D. p21 is a universal inhibitor of cyclin kinases. Nature 1993;366:701–4.
22. Peng CY, Graves PR, Thoma RS, Wu Z, Shaw AS, Piwnica-Worms H. Mitotic and G2 checkpoint control: regulation of 14–3-3 protein binding by phosphorylation of Cdc25C on serine-216. Science 1997;277:1501–5.
23. Herman-Antosiewicz A, Singh SV. Checkpoint kinase 1 regulates diallyl trisulfide-induced mitotic arrest in human prostate cancer cells. J Biol Chem 2005;280:28519–28.
24. Kumagai A, Dunphy WG. Binding of 14–3-3 proteins and nuclear export control the intracellular localization of the mitotic inducer Cdc25. Genes Dev 1999;13:1067–72.
25. Xiao D, Herman-Antosiewicz A, Antosiewicz J, et al. Diallyltrisulfide-induced G(2)-M phase cell cycle arrest in human prostate cancer cells is caused by reactive oxygen species-dependent destruction and hyperphosphorylation of Cdc 25 C. Oncogene 2005;24:6256–68.
26. Geiszt M, Kopp JB, Varnai P, Leto TL. Identification of renox, an NAD(P)H oxidase in kidney. Proc Natl Acad Sci U S A 2000;97:8010–4.
27. Serrano M, Lee H, Chin L, Cordon-Cardo C, Beach D, DePinho RA. Role of the INK4a locus in tumor suppression and cell mortality. Cell 1996;85:27–37.
28. Curtin JA, Fridlyand J, Kageshita T, et al. Distinct sets of genetic alterations in melanoma. N Engl J Med 2005;353:2135–47.
29. Takata M, Saida T. Genetic alterations in melanocytic tumors. J Dermatol Sci 2006;43:1–10.
30. Murakami S, Noguchi T, Takeda K, Ichijo H. Stress signaling in cancer. Cancer Sci 2007;98:1521–7.